Low-Cost Measurement of Electromagnetic Leakeage in Domestic Appliances Using Software-Defined Radios

Marcelo B. Perotoni*1 ⓘ, Lincoln Ferreira1, Alexandre Maniçoba2

1Universidade Federal do ABC, Santo André, SP, Brasil.
2Instituto Federal de São Paulo, Cubatão, SP, Brasil.

Concerns regarding long-term effects of stray electromagnetic fields emitted by household appliances have been usually covered by mainstream and social media outlets, even though biomedical exposure studies have conclusions leaning towards low-risks. The quick deployment of Internet of Things (IoT) shows that the number of connected devices is likely to increase even more. Though most systems operate with very low-amplitude field levels, the coexistence of several different devices and continuous operation near the human body is seen as a possible cause of illnesses, particularly in children. This study shows a method of addressing fields at the 2450-MHz range using low-cost and easily constructed devices, based on a software-defined radio operating as a receiver. It allows the investigation of hot spots inside residential or office areas, with measured amplitude field levels found after proper conversion using the sensor antenna factor.
Keywords: Antenna, electromagnetic interference, software-defined radio.

1. Introduction

Widespread use of wireless systems and other domestic appliances have become a source of concerns regarding health effects of their emitted radiated fields [1]. Since both electric and magnetic fields (EMF) are invisible, their exposure is not felt by humans and actual long-term effects are still discussed in the biophysical scientific literature, with disputed conclusions due to the inherent complexity of their evaluation and other related issues, such as non-ideal control cases, confounding and bias [2]. In particular, cancer, leukemia, and brain diseases are the main concern behind long-term EMF exposure with actual field dosimetry being a natural obstacle in humans [3], therefore only experiments with mice or in-vitro evaluations are possible, or by the use of electromagnetic simulation. Signals whose frequencies are below UV (ultraviolet) light (800 THz) are considered non-ionizing radiation since their energies are below the required threshold to effect atomic levels [4]. Non-ionizing radiation, in principle, only heats up tissues and are not hazardous, even used for therapeutic treatments (ablation) [5].

ICNIRP (International Commission on Non-Ionizing Radiation Protection) have beenn setting the standards and limits for safe field levels, from static regimes up to 300 GHz [6]. It contains descriptions of the mechanisms and hypotheses behind the human effects, for instance:

- Fields whose frequencies vary between 100 kHz and 20 MHz have strong absorption in the legs and neck;
- from 20 MHz to 300 MHz the absorption takes place in the whole body, with occasional localized resonances (e.g., head) which might generate high amplitude fields;
- from 300 MHz up to several GHz absorption is local and non-uniform.

ICNIRP standards are valid globally, however, Eastern European guidelines contemplate chronic exposures and are usually more conservative, sometimes orders of magnitude lower [7]. With regard to household and ordinary daily activities, fields are generated mostly with some frequencies ranges:

- 60 or 50 Hz AC utility frequency, which generate quasi-static fields due to high currents circulating in appliances such as welding machines, vacuum cleaners, induction stoves, etc;
- mobile phones which operate in the frequencies of 700 MHz, 840 MHz, 1800 MHz, and 2600 MHz, depending on the country and service provider;
- WiFi (IEEE 802.11) networks currently operate in 2450 MHz and 5800 MHz. Due to its popularity in tablets, laptops, Smart TVs and mobile phones, users need to ensure a good coverage in the domestic environment, sometimes using boosters to amplify it;
- Bluetooth shares the 2450 MHz range with WiFi, and it is oriented towards short-range communication, usually with lower power levels;

---

* Correspondence email address: marcelo.perotoni@ufabc.edu.br

- domestic microwave ovens, using high-power vacuum tubes oscillating at 2450 MHz.

Worth mentioning items are overhead power lines (60 or 50 Hz), source of concerns regarding children leukemia and brain tumors [8], and mobile phone base stations located near residential areas [9]. They are, however, present only in some specific locations, making it easier the tracking of long-term health problems. In the literature, EMF emitted by an induction cooker in a residential area, frequencies up to 50 kHz, was investigated using simulation and magnetic field measurements [10]. A commercial Gaussmeter, frequency range up to 10 kHz, tested domestic appliances in India and found out largest stray field amplitudes around computers [11]. Similar studies were performed in Bangladesh, where some equipment was found to exceed threshold limits [12]. It is also reported the evaluation of magnetic and electric fields of either domestic and occupational locations, such as substations and busbars [13]. A professional GTEM (Gigahertz-Transverse Electromagnetic Cell) was used to investigate magnetic radiation emitted from some appliances with DC motors, from 9 kHz to 1 GHz, so that a juicer and a mincer were found to exceed EN5501 emission thresholds [14]. These concerns motivated specific architecture guidelines to reduce radiation levels in household environments, with suggestions such as the use of green plants and metallic materials as EMF shields [15].

From the Physics viewpoint, radiated energies are divided in near-field (NF) or far-field (FF), considering the distance from the emission source. The former criterion is also called quasi-static, since fields within this area have its formulation resembling DC (static) cases, whereas the latter actually deals with electromagnetic waves, whose Electric (E) and Magnetic Fields (H) are spatially orthogonal and mutually coupled. NF's in turn, are uncoupled, and the choice upon E or H fields depends on the source; H is usually radiated by current sources, with inductive nature, whereas E arises from high-voltages (with capacitive characteristic). The separation between both NF and FF regions has several different definitions, among them $\lambda/2\pi$ [16] or $2D^2/\lambda$ [17]; where D is the largest dimension of the antenna and λ the signal wavelength. Proposed guidelines consider NF in households eminently of magnetic nature, since most sources are transformers, electric motors, ballasts, etc, which have inductive characteristics. Unfortunately, shielding against low-frequency magnetic fields is complicated [16], so when needed it might require cumbersome thick metallic layers.

This study presents an affordable way to address quantitatively and qualitatively, in case calibration is performed, EMF using probes. Results herein obtained are not related to any health hazard conclusion, they rather focus on the experimental engineering aspect of it. Figure 1 shows the idea, an NF or FF probe samples the existing field and the receiving signal is read by an SDR
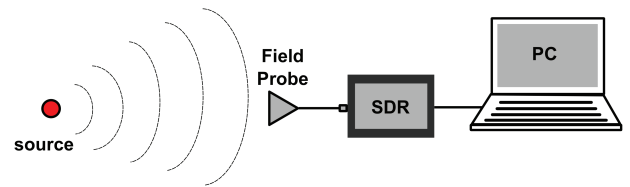

Figure 1: Block diagram of the measurement instrument.

(Software-Defined Radio), connected to a laptop running an application displaying frequency and amplitude data. It is a low-cost alternative to professional-grade instruments, and permits measuring domestic and industrial environments, using easily available materials and open-source software applications. In contrast to broadband readings [12], [13], whose identification of the frequency is not possible, the SDR enables a spectrum analysis where the exact emitted frequency can be tracked, as well as its temporal distribution, in case of bursts or transients.

NF and FF probes are presented, particularly with details concerning the conversion of received power into field amplitudes for the case of a monopole antenna, which was designed, constructed, and measured. This class of antenna was chosen due to its easy construction, and is used as an FF probe in a domestic environment with two subjects - a wireless router and a microwave oven. Details of the software application are discussed, based on an free and open-source tool.

2. NF e FF Probes

A fundamental problem related to fields measurements using probes or antennas is the relation between their received voltage or power at their respective terminals and the absolute field value sampled by the device. It is clear that the very presence of the measuring device disturbs the local field pattern, thereby introducing an initial error to the process. That is the first difference between the concept of antenna and probe; the former is designed to operate in far-field conditions, and is usually resonant, i.e., with an optimal response within a certain frequency range, which, due to the Reciprocity Theorem [18], implies creating a strong coupling to the transmitting source. On the other hand, a near-field probe, due to its non-resonant characteristic, introduces less coupling to the existing field. Besides it, within NF regime both electric and magnetic fields are uncoupled, so it is necessary to have different probes, usually loops for magnetic and dipole-like for electric fields [19].

In the case of an antenna used as Far-Field probe the AF (Antenna Factor) is defined as [17]:

$$AF = \frac{E_i}{V_{rec}} \tag{1}$$

where E_i is the existing electric field, units V/m, and V_{rec} represents the received voltage (units V) in the

antenna terminals. AF unit, therefore, is $1/m$. Since the antenna operates in the far-field, there is a TEM-type wave with both electric and magnetic fields orthogonally displaced in space, so the power density S, or Poynting vector, can be expressed by the relation:

$$\vec{S} = \vec{E} \times \vec{H}^* = \frac{|E|^2}{\eta_o} \tag{2}$$

where η_o is the free-space impedance (377 Ω). The goal is to determine the AF from the antenna gain G. For that, it is used the received power P_{rec}, defined after the power density and the antenna effective aperture A_e:

$$P_{rec} = S \cdot A_e = \frac{|E|^2}{\eta_o} \frac{G}{\frac{4\pi}{\lambda^2}} = \sqrt{\frac{cE}{f}} \frac{G}{4\pi\eta_o} \tag{3}$$

with f representing the frequency and c the speed of light. The voltage is related to the power by means of the reference impedance Z_o, usually 50 Ω:

$$V = \sqrt{\frac{P_{rec}}{Z_o}} \tag{4}$$

Combining (3) and (4) it is possible to define AF as:

$$AF = \sqrt{\frac{4\pi\eta_o f^2}{GZ_o c^2}} \tag{5}$$

upon grouping the constants and leaving out only the variables frequency and gain, using decibels:

$$AF_{dB} = 20\log f - G_{dB} - 149.7 \tag{6}$$

where both AF_{dB} and G_{dB} are expressed in dB. Therefore, with only gain information it is possible to estimate the absolute field value at the antenna position.

Similar procedure is applied when the AF for a NF probe is needed, replacing the gain by other parameter. A common method involves the calibration of the NF probe after the measurement of a TEM-type structure (wire or microstrip line over a ground plane), whose modeling allows exact analytical field expressions [20]. By relating the computed power or voltage at the NF probe terminals with the analytical field value the AF is univocally determined. In case of loops, comparison with the Faraday law allows the conversion and determination of AF in lower frequency ranges, with a series-resistor sampling the exciter resistor in the loop by an oscilloscope [21].

3. Monopole Antenna as a Probe

For the sake of measurement, a monopole antenna was built and simulated, so that its AF can be computed and used as a field sensor in the FF, shown in Fig. 2. The monopole was chosen due its easy construction and its feeding method, which unlike dipoles does not

require any type of balun to convert from common unbalanced connections, usually found in SDRs and other instruments. Its simulation included an SMA coaxial connector, to ensure a more realistic model. Figure 3 shows the computed and measured S11 parameters, alongside the simulated gain. The antenna was designed using CST Microwave Studio transient solver, and the measurement agrees with the computed results, the oscillations seen on the curve are ascribed to cable reflections. The monopole operates from 2.16 to 2.6 GHz, following the convention of reflection losses smaller than 10 dB. Since a professional shielded environment for the antenna measurement is not available, the gain G_{dB} is considered from the simulation, since it provided consistent results when considered the reflection measurements. Computed G_{dB} factor is later inserted in eq. (6), shown in Fig. 4.
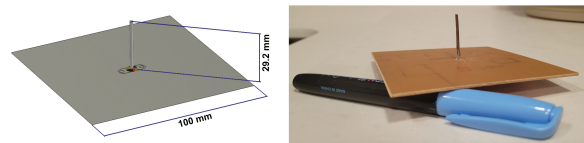

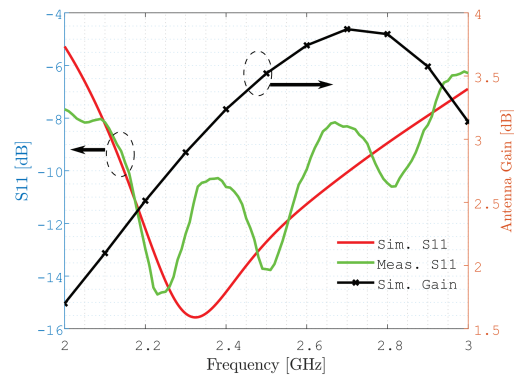**Figure 2:** Monopole in the simulation (left) and actual prototype (right).

Figure 3: Computed and measured S11 with the simulated antenna gain.
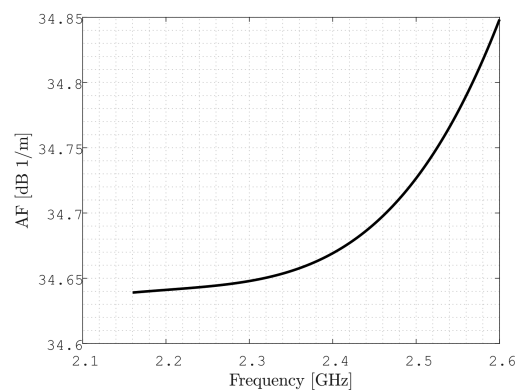

Figure 4: Antenna Factor of the constructed monopole.

4. Software Application and SDR Interface

Time-domain samples acquired by the SDR (HackRF One) are received by the USB port and transferred to GNU Radio. Figure 5 shows the GNU Radio block diagram that is responsible for measuring the spectrum. It is very clean and simple, containing the block responsible for control and interface to the SDR (named osmocom Source, left); a throttle in yellow (to decrease the data traffic otherwise only hardware-constrained); a DC blocker to eliminate zero-IF leaking and two plotting blocks, a Frequency-type (similar to spectrum analyzers) and waterfall. GNU Radio has, however, many other blocks that can be used, such as filters, TCP/IP (ZeroMQ) bridges to other clients, data processing and recording, etc.

The choice of the hardware (SDR) involves some points to ponder:

- Number of bits of its analog-to-digital converter (ADC), impacts on the sensitivity of the receiver [22]. Low-cost units are based on 8-bits ADCs, whereas high-end SDRs usually employ 12-bits converters.
- The frequency to be analyzed has to be within SDR operating range. They usually start around tens of MHz, extending up to the GHz range.
- Price range depends on the number of available RF channels. Receiving-only units are the cheapest, with high-end SDRs containing full-duplex independent RF channels.
- Software interface is a critical issue. Some units depend on commercial software, others are easily interfaced with free GNU Radio or Python. Access to this software application package is, usually, easier with Linux than Windows operational systems (OS). Unfortunately, there is no way to tell ahead of time if the chosen SDR is going to work with the particular OS version, it depends on installed drivers and local settings, so tweaking is oftentimes necessary.

- Instantaneous bandwidth is also defined by the ADC contained in the SDR. A larger bandwidth implies that a wider band can be covered at once, so fast transients can be picked up. This is one of the greatest drawbacks of SDRs in contrast to commercial spectrum analyzers, which allow a full-bandwith coverage at once. Monitoring larger bandwidths with SDRs involve some form of sequentially switching the central frequency.

One of the most popular SDRs is the RTL, a low-cost, receiver-only 8-bits ADC unit, similar to a common USB dongle [23]. Due to its popularity, it is interfaced by several different software suites, such as Matlab, Python, GNU Radio, and customized applications developed specifically for it. Its upper frequency, however, is 1700 MHz, so WiFi signals or microwave ovens leaking radiation is beyond its range. It also has a small bandwidth, 2 MHz.

For this specific study, an 8-bit half-duplex HackRF One was employed, since its upper-frequency range lies around 6 GHz, so adequate for investigating signals in both 2.4 GHz and 5.8 GHz bands. Due to its open-source design, cheaper clone boards are available, which operate with GNU Radio or Python commands. Its 20-MHz instantaneous bandwidth allows convenient visualization of transients.

If the lower kHz range is to be investigated, SDRs based on the SRP unit start out around 10 kHz to 100 KHz, so emissions from this range can be measured. Another alternative is the use of down-converter circuits cascaded between the antenna or probe and the SDR, commercially available with relative low costs. RSP and its clones are also interesting due to their 12-bits ADC, which guarantees a nominal theoretical 24-dB dynamic range above the 8-bits HackRF One.

5. Measurements

Microwave ovens are chosen to be studied due to their high power and almost universal domestic presence since initially introduced in 1945 [24]. They are designed to
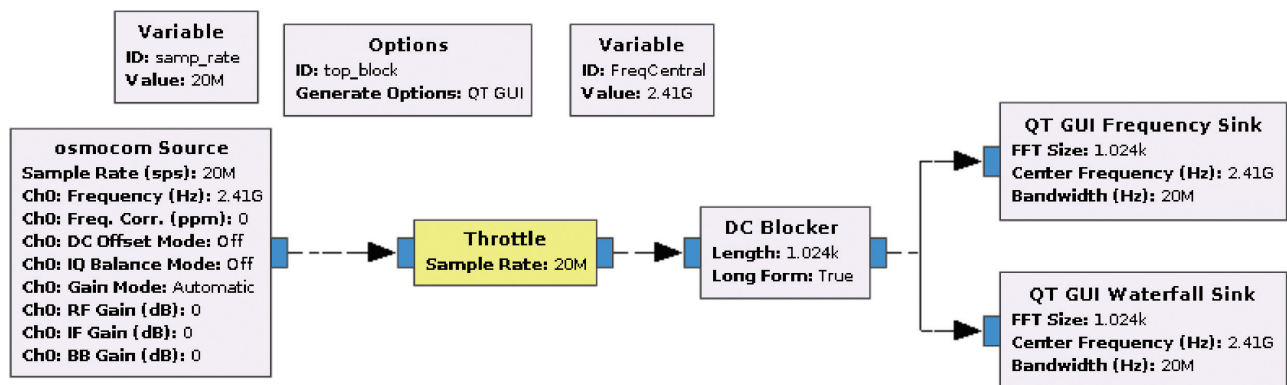

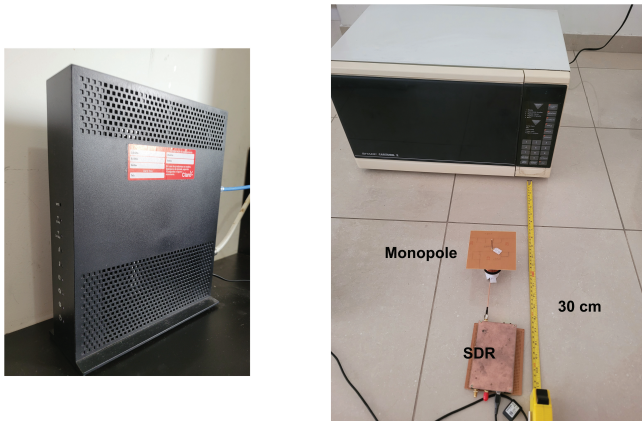**Figure 5:** GNU Radio program to show frequency domain measurements acquired by the probe or antenna.

Figure 6: Measured appliances, wireless router (left) and microwave oven (right).

Figure 7: Measurements of two domestic appliances, left power in dBm and right, after conversion, electric field in dBmV/m.

Figure 8: Waterfall plot for the spectrum distribution of the microwave oven (top) and router (bottom).

avoid energy leaking when their door is closed [4], using resources such as shielding and serrated chokes [25], however, it is unlikely all makers and old models comply to this requirement. Besides domestic usage, high-powered units can be used in restaurants and confined in tight spaces inside airliners, a specific case analyzed elsewhere with simulation [26].

Two appliances were measured, a 1200-W microwave oven (Sharp Carousel II) and a wireless router (SAGEM-COM F@ST3486), shown in Fig. 6. The wireless router was chosen due to its overall domestic and office presence and also as a comparison with the oven since both share the same frequency range. The monopole antenna was kept 30 cm from the equipment, and each 20-MHz bandwidth had its power acquired during 1 minute using the Max-Hold option within the GNU Radio plot, to register the maxima. Considering the 2450 MHz frequency, the limit between NF and FF is approximately 2 cm according to [16] and 15 cm [17], so the monopole was, for both criteria, within the FF region.

Since received power amplitudes were close to 0 dBm, the LNA amplifier was switched off in order to avoid RF frontend overload. Figure 7 contains both P_{rec} and Electric field, for both devices. After the measurement, conversion to electric field amplitude values is performed, following (7). Variables are indicated with the respective units.

$$E_{dBmV/m} = AF_{dBm^{-1}} + P_{recdBm} - 30 - 20\log\sqrt{50} + 30 \tag{7}$$

The last (30) factor corresponds to transformation from dBv/m to dBmV/m whereas the middle (-30) term brings the received power from dBm to dBW. Most spectrum analyzers and software-defined radios display power units in dBm, so the aforementioned conversion is direct.

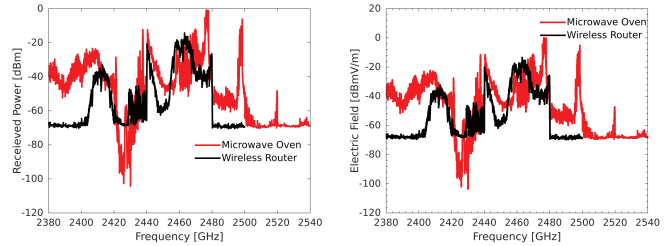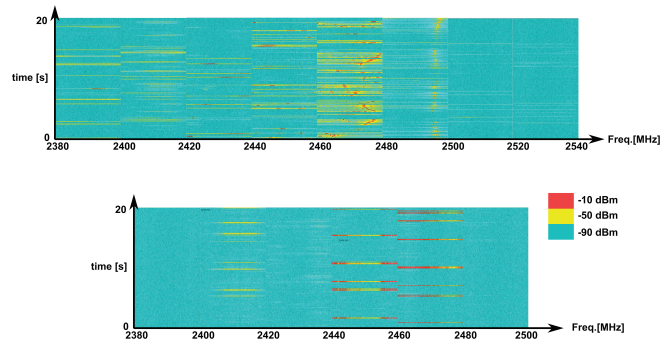The maximum observed field value was 0.032 V/m, at 2476 MHz, emitted by the microwave oven. It is

significantly smaller than those observed elsewhere [7], which had 2.5 V/m at a distance of 0.5 m. Results are much below ICNIRP guidelines for the 2.4 GHz range [6], 61.4 V/m for the general public and 173.66 V/m for controlled environments.

Waterfall plots show the spectrum distribution along the time. Figure 8 shows measurements during 20 secs for each sequential 20-MHz bandwidth, for both microwave oven and router. The acquired data does not correspond to the ones shown in Fig. 7, they belong to another set of measurements. It is possible to see the stochastic distribution of emitted radiation in the microwave oven, in contrast to the router, particularly in the 2460 MHz to 2480 MHz range.

6. Conclusion

This article reported a low-cost system to evaluate stray electromagnetic fields, based on SDRs, enabling a solution for addressing a common source of concern without special instrumentation. A monopole antenna was designed and characterized as field-probe, for farfield conditions, after its Antenna Factor was computed from its simulated gain. Two domestic equipment, a microwave oven, and a wireless router had their EMF measured with the proposed system. A similar procedure can be followed for measuring signals in lower frequency ranges, using probes instead of antennas.

References

[1] M. Röösli, Therapeutische Umschau **70**, 12 (2013).

[2] M. Röösli, *Epidemiology of Electromagnetic Fields* (CRC, Boca Raton, 2014).

[3] R. Stepanski, O. Janh and J. Zeitlhofer, Acta Med. Austriaca **27**, 3 (2000).

[4] A. Zamanian and C. Hardiman, High Frequency Electronics **July**, 16 (2005).

[5] C.J. Simon, D.E. Dupuy and W.W. Mayo-Smith, Radio Graphics **25**, s69 (2005).

[6] ICNIRP, Health Physics **74**, 494 (1998).

[7] P. Lopez-Iturri, S. Miguel-Bilboa, E. Aguirre, L. Azpilicueta, F. Falcone and V. Ramos, BioMed Research International **2015**, 603260 (2015).

[8] P. Gajŝek, P. Ravazzani, J. Grellier, T. Samaras, J. Bakos and G. Thuróczy, International Journal of Environmental Research and Public Health **13**, 875 (2016).

[9] V.G. Khurana, L. Hardell, J. Everaert, A. Bortkiewicz, M. Carlberg and M. Ahonen, International Journal of Occupational and Environmental Health **16**, 263 (2016).

[10] D. Medved and O. Hirka, Acta Electrotechnica et Informatica, **17**, 48 (2017).

[11] K.S. Prashanth, T.R.S. Chouhan and S. Nadiger, in *IET-UK International Conference on Information and Communication Technology in Electrical Sciences* (ICTES, Chennai 2007).

[12] M. Haque, M. Quamruzzaman and S. Haque, ARPN Journal of Engineering and Applied Sciences **13**, 4976 (2018).

[13] H. Li, L. Li, K. Zhang, Y. Liu, Y. Wang, Y. Shen and C. Xiong, in *IEEE 3rd Advanced Information Management,Communicates,Electronic and Automation Control Conference* (IMCEC, Chongqing, 2019).

[14] J. Michalowska, A. Tofil and J.Józwik, in *International Conference Applications of Electromagnetics in Modern Engineering and Medicine* (Janów Podlaski, 2019).

[15] Z. Zou, W. Hu and Y. Wang, in *9th International Conference on Computer-Aided Industrial Design and Conceptual Design* (Beijing, 2008).

[16] H.W. Ott, *Electromagnetic Compatibility Engineering* (Wiley, Hoboken, 2009).

[17] C.R. Paul, *Introduction to Electromagnetic Compatibility* (Wiley, Hoboken, 2006).

[18] C.A. Balanis, *Modern Antenna Handbook* (Wiley, Hoboken, 2008).

[19] P. Bienkowski and H. Trzaska, *Electromagnetic Measurements in the Near Field* (Scitech, Raleigh, 2012).

[20] T. Dimitrijević, A. Atanaskovic, N.S. Dončov, D.W.P. Thomas, C. Smartt and M.H. Baharuddin, IInternational Journal of Microwave and Wireless Technologies **12**, 878 (2020).

[21] W.G. Fano, R. Alonso and L.M. Carducci, in *IEEE Global Electromagnetic Compatibility Conference* (GEMCCON, La Plata, 2016).

[22] A. Heuberger and E. Gamm, *Software Defined Radio-Systeme für die Telemetrie* (Springer Vieweg, Berlin, 2017).

[23] R.W. Stewart, K.W. Barlee, D.S.W. Atkinson and L.H. Crockett, *Software Defined Radio Using MATLAB® & Simulink® and the RTL-SDR* (Strathclyde Academic Media, Glasgow, 2017).

[24] J.M. Osepchuk, in *IEEE MTT-S International Microwave Symposium Digest* (Boston, 2009).

[25] K. Tomiyasu, IEEE Microwave Magazine **9**, 206 (2008).

[26] S. Narayan, K. Arun, R.M. Jha and J.P. Bommer, in *Proceedings of the 2012 IEEE International Symposium on Antennas and Propagation* (Chicago, 2012).